

Nuclear Forces and Nuclear Structure ¹

R. Machleidt

Department of Physics, University of Idaho, Moscow, Idaho 83844
Electronic address: machleidt@uidaho.edu

Abstract. After a historical review, I present the progress in the field of realistic NN potentials that we have seen in recent years. A new generation of very quantitative (high-quality/high-precision) NN potentials has emerged. These potentials will serve as reliable input for microscopic nuclear structure calculations and will allow for a systematic investigation of off-shell effects. The issue of three-nucleon forces is also discussed.

INTRODUCTION

The goal of nuclear physics is to explain the properties of atomic nuclei in fundamental terms—where the stress is on *fundamental*. The debate then begins with what the fundamental ingredients (or ‘first principles’) are from which we should start. Nuclear physics is strong interaction physics, so, based upon the Standard Model, it should be quarks exchanging gluons. However, in the spirit of the currently fashionable effective field theories, one may argue that any theory is effective, and what theory is appropriate depends on the energy scale. In fact, Weinberg [1] pointed out 20 years ago that an effective field theory of nucleons and mesons that observes the same symmetries as QCD is equivalent to QCD. This allows us to consider mesons and nucleons as the basic items, on our energy scale. The spin-off from the mesons is the nuclear force.

Thus, it is suggested that the appropriate fundamental ingredients that nuclear structure should be based upon are nucleons and the ‘fundamental’ nucleon-nucleon (NN) interaction (created by meson exchange). The above discussion also provides clear guideline for how to extend the model if it fails. One may introduce explicit meson degrees of freedom and one may complement the nucleon by meson-nucleon resonances (e.g., the $\Delta(1232)$ isobar); moreover, one may take into account the quark substructure of nucleons. However, it should be stressed that the starting point—besides being fundamental—must also be simple. Nucleons interacting via the two-nucleon force is the simplest of all basic pictures. Only where we have clear evidence that this frame work is insufficient may we extend it. For most problems of conventional nuclear structure, we do not have such evidence at this time.

Starting from nucleons and the bare two-nucleon force, any nuclear many-body problem one may consider is exactly defined. However, due to limitations in computing power, the problem can be solved exactly only up to $A = 8$ [2], and since the needed computing time goes up as factorial of A , there is little hope that we will ever get beyond $A = 12$. Therefore, in most problems of nuclear structure and reactions, the first step is to derive an effective interaction from the bare NN potential. Usually, this involves Brueckner theory or some variation/extension thereof [3,4]. However, it is important to stress that—no matter what many-body theory or model is used—this step has to be done in a *parameter-free* way. Finally, the effective interaction may be applied in the shell model, yielding predictions for nuclear properties.

Following this scheme (which is known as *microscopic* nuclear structure), the predictions depend only on two fundamental items: the bare NN potential and the nuclear many-body theory/model applied. Thus, the comparison of the predictions with the data will allow for conclusions concerning the NN potential (off-shell) and the appropriate nuclear many-body theory. In other words, we will learn something about the foundations of our profession, which is our ultimate goal.

In this conference, we have many contributions that deal with particular effective interactions, shell-model applications, predicted and measured nuclear properties. It is the purpose of this contribution to fill-in on one of the fundamental ingredients that is at the outset of all this, namely, the NN interaction. As it turns out, we have had substantial progress in recent years and—as a result of this—the starting conditions for *microscopic* nuclear structure calculations are better than ever.

¹⁾ Invited Talk presented at the *Nuclear Structure '98* conference, Gatlinburg, Tennessee, August 10-15, 1998.

To put the recent advances into perspective, I will start with a brief historical review and then present the new developments. Artificially, I will draw the line between ‘history’ and recent progress/new developments in the year of 1990.

HISTORICAL PERSPECTIVE

Here, I will give a brief summary of the status in the field of nuclear forces before 1990.² This will make it easier for us to appreciate the progress of the past eight years. Historically, one may distinguish between three decades of work on the meson theory of nuclear forces, namely, the 60’s, 70’s, and 80’s. Each decade is characterized by progress in a particular sector of meson theory, namely, the one-boson-exchange model, the two-pion exchange contribution to the NN interaction, and contributions beyond 2π , respectively.

The One-Boson-Exchange Model

The first quantitative meson-theoretic models for the NN interaction were the one-boson-exchange potentials (OBEP). They emerged right after the experimental discovery of heavy mesons in the early 1960’s. In general, about six non-strange bosons with masses below 1 GeV are taken into account: the pseudoscalar mesons $\pi(138)$ and $\eta(549)$, the vector mesons $\rho(769)$ and $\omega(783)$, and two scalar bosons $a_0/\delta(983)$ and $\sigma(\approx 550)$. The first particle in each group is isovector (isospin $I = 1$) while the second is isoscalar ($I = 0$). The pion provides the tensor force, which is reduced at short range by the ρ meson. The ω creates the spin-orbit force and the short-range repulsion, and the σ is responsible for the intermediate-range attraction. Thus, it is easy to understand why a model which includes at least four mesons can reproduce the major properties of the nuclear force.³

A classic example for an OBEP is the Bryan-Scott potential published in 1969 [7]. Since it is suggestive to think of a potential as a function of r (where r denotes the distance between the centers of the two interacting nucleons), the OBEP’s of the 1960’s were represented as local r -space potentials. To reduce the original one-meson-exchange Feynman amplitudes to such a simple form, drastic approximations have to be applied. The usual method is to expand the amplitude in terms of p^2/M and keep only terms up to first order (and, in many cases, not even all of them). Commonly, this is called the *nonrelativistic OBEP*. Besides the suggestive character of a local function of r , such potentials are easy to apply in r -space calculations. However, the original potential (Feynman amplitudes) is nonlocal, and, thus, has a very different off-shell behaviour than its local approximation. Though this does not play a great role in two-nucleon scattering, it becomes important when the potential is applied to the nuclear few- and many-body problem. In fact, it turns out that the original nonlocal potential leads to much better predictions in nuclear structure than the local approximation (see below).

Historically, one must understand that after the failure of the pion theories in the 1950’s, the one-boson-exchange (OBE) model was considered a great success in the 1960’s. However, there are conceptual and quantitative problems with this model.

A questionable point of the OBE model is the fact that it has to introduce a scalar-isoscalar σ -boson in the mass range 500–700 MeV, the existence of which is controversial (for a current status report, see Ref. [8]). Furthermore, the model is restricted to single exchanges of bosons that are ‘laddered’ in an unitarizing equation. Thus, irreducible multi-meson exchanges, which may be quite sizable (see below), are neglected.

Quantitatively, a major drawback of the *nonrelativistic* OBE model is its failure to describe certain partial waves correctly. The Bryan-Scott nonrelativistic OBE potential predicts 1P_1 and 3D_2 phases substantially above the data. [9]

An important advance during the 1970’s has been the development of the *relativistic OBEP* [10]. In this model, the full, relativistic Feynman amplitudes for the various one-boson-exchanges are used to define the potential. These nonlocal expressions do not pose any numerical problems when used in momentum space.⁴ The quantitative deficiencies of the nonrelativistic OBEP disappear when the non-simplified, relativistic, nonlocal OBE amplitudes are used.

The *Nijmegen potential* [11], published in 1978, is a nonrelativistic r -space OBEP. As a latecomer, it is one of the most sophisticated examples of its kind. It includes all non-strange mesons of the pseudoscalar, vector, and scalar nonet. Thus, besides the six mesons mentioned above, the $\eta'(958)$, $\phi(1020)$, and $S^*(993)$ are taken into account. The

²⁾ A more comprehensive historical account is given in Refs. [5,6].

³⁾ The interested reader will find a detailed, pedagogical introduction into the OBE model in sections 3 and 4 of Ref. [5].

⁴⁾ In fact, in momentum space, the application of a nonlocal potential is numerically as easy as using the momentum-space representation of a local potential.

model also includes the dominant $J=0$ parts of the Pomeron and tensor (f , f' , A_2) trajectories, which essentially lead to repulsive central Gaussian potentials. For the Pomeron (which from today's point of view may be considered as a multi-gluon exchange) a mass of 308 MeV is assumed. However, this potential is still defined in terms of the nonrelativistic local approximations to the OBE amplitudes. Therefore, it shows exactly the same problems as its ten years older counterpart, the Bryan-Scott potential: the Nijmegen potential fails to predict the 1P_1 and 3D_2 phase shifts correctly to the same extent as the Bryan-Scott potential. In addition, the Nijmegen potential overpredicts the 3D_3 phase shifts by more than a factor of two [9], a problem the models of the 1960's did not have. The inclusion of more bosons does obviously not improve the model and is, thus, unnecessary. It is more important to calculate the one-boson exchange amplitudes correctly and without the local approximations.

The 2π -Exchange Contribution to the NN Interaction

In the 1970's, work on the meson theory of the nuclear force focused on the 2π -exchange contribution to the NN interaction to replace the σ -boson. One way to calculate these contributions is by means of dispersion relations. Around 1970, many groups throughout the world were involved in this approach; we mention here, in particular, the Stony Brook [12] and the Paris [13] groups. These groups could show that the intermediate-range part of the nuclear force is, indeed, described correctly by the 2π -exchange as obtained from dispersion integrals.

To construct a complete potential, the Stony Brook as well as the Paris group complemented their 2π -exchange contribution by one-pion-exchange (OPE) and ω exchange. In addition to this, the Paris potential [14] contains a phenomenological short-range potential for $r < 1.5$ fm.

In microscopic nuclear structure calculations, the off-shell behavior of the NN potential is important. The fit of NN potentials to two-nucleon data fixes them only on-shell. The off-shell behavior cannot, in principle, be extracted from two-body data. Theory could determine the off-shell nature of the potential; however, not every theory can do that. Dispersion theory relates observables (equivalent to on-shell T -matrices) to observables; e. g., πN data to NN data. Thus, dispersion theory cannot, in principle, provide any off-shell information. The Paris potential is based upon dispersion theory; thus, the off-shell behavior of this potential is not determined by the underlying theory. On the other hand, every potential does have an off-shell behavior. When undetermined by theory, then the off-shell behavior is a silent by-product of the parametrization chosen to fit the on-shell T -matrix, with which the potential is identified. In summary, due to its basis in dispersion theory, the off-shell behaviour of the Paris potential is not derived on theoretical grounds. This is a serious drawback when it comes to the question of how to interpret nuclear structure results obtained with this potential.

The Field-Theoretic Approach to 2π -Exchange

In a field-theoretic picture, the interaction between mesons and baryons is described by effective Lagrangians. The NN interaction can then be derived in terms of field-theoretic perturbation theory. The lowest order (that is, the second order in terms of meson-baryon interactions) are the one-boson-exchange diagrams, which are easy to calculate.

More difficult (and more numerous) are the irreducible two-meson-exchange (or fourth order) diagrams. It is reasonable to start with the contributions of longest range. These are the graphs that exchange two pions. There are two complications that need to be taken into account: meson-nucleon resonances and meson-meson scattering. The lowest πN resonance, the so-called Δ isobar with a mass of 1232 MeV, gives rise to one set of diagrams. The other set involves $\pi\pi$ interactions. Since it is well established that two pions in relative P -wave form a resonance (the ρ meson), there is no problem with ρ exchange. However, the existence of a proper resonance in $\pi\pi - S$ -wave below 900 MeV is controversial [8]. In any case, there are strong correlations between two pions in S -wave at low energies. Durso *et al.* [15] have shown that these correlations can be described in terms of a broad mass distribution of about 600 ± 260 MeV, which in turn can be approximated by a zero-width scalar-isoscalar (σ) boson of mass 550 MeV [16].

In summary, two approaches are available for calculating the 2π -exchange contribution to the NN interaction: dispersion theory (Paris [13,14]) and field theory (Bonn [16]). One can compare the predictions by the two approaches with each other as well as with the data. For this purpose, one looks into the peripheral partial waves of NN scattering. By and large, one finds satisfactory agreement [16].

TABLE 1. Comparison of some typical meson-theoretic nucleon-nucleon models of the pre-1990 era.

	Nijmegen(1978) [11]	Paris Potential(1980) [14]	Bonn full model(1987) [16]
# of free parameters	15	≈ 60	12
Theory includes:			
OBE terms	Yes	Yes	Yes
2π exchange	No	Yes	Yes
$\pi\rho$ diagrams	No	No	Yes
Relativity	No	No	Yes
χ^2/datum for fit of world NN data:			
pp data	2.06	2.31	1.94
np data	6.53	4.35	1.88
pp and np data	5.12	3.71	1.90

$\pi\rho$ -Contributions and the Bonn Potential

A model consisting of $\pi + 2\pi + \omega$ describes the peripheral partial waves quite satisfactory. However, when proceeding to lower partial waves (equivalent to shorter internucleonic distances), this model generates too much attraction. This is true for the dispersion-theoretic (Paris) as well as the field-theoretic (Bonn) result. Obviously, further measures have to be taken at short range to arrive at a quantitative model for the NN interaction. It is at this point that the philosophies of the Bonn and Paris groups diverge.

The Paris group decided to give up meson theory at this stage and to describe everything that is still missing by phenomenology. Thus, they added a phenomenological short-range potential for $r < 1.5$ fm which requires many parameters (see Table 1, below) that do not allow for a clear-cut physical interpretation. This short-range potential affects the S-, P-, and D-waves of NN scattering which are, therefore, largely a product of phenomenology in the Paris model.

In contrast, the Bonn group continued to consider further irreducible two-meson exchanges. The next set of diagrams to be considered are the exchanges of π and ρ . As it turns out, these contributions very accurately take care of the discrepancies that remained between theory and experiment [16].

Thus, the $\pi\rho$ contributions provide the short-range repulsion which was still missing. It is important to note that the $\pi\rho$ contributions have only one free parameter, namely the cutoff for the $\rho N\Delta$ vertex. The other parameters involved occur also in other parts of the model and were fixed before (like the πNN and ρNN coupling constants and cutoff parameters). Notice also that the $\pi N\Delta$ and $\rho N\Delta$ coupling constants are not free parameters, since they are related to the corresponding NN coupling constants by $SU(3)$.

In summary, a proper meson-theory for the NN interaction should include the irreducible diagrams of $\pi\rho$ exchange. This contribution has only one free parameter and makes comprehensive short-range phenomenology unnecessary. Thus, meson theory can be truly tested in the low-energy NN system.

In the 1970's and 80's, a field-theoretic model for the NN interaction was developed at the University of Bonn. This model consists of single π , ω , and a_0/δ exchange, the field-theoretic 2π model, and $\pi\rho$ diagrams, as well as a few more irreducible 3π and 4π diagrams (which are not very important, but indicate convergence of the diagrammatic expansion). This quasi-potential has become known as the 'Bonn full model' [16]. It has 12 parameters which are the coupling constants and cutoff masses of the meson-nucleon vertices involved. With a reasonable choice for these parameters, a very satisfactory description of the NN observables up to 300 MeV is achieved (see Table 1). Since the goal of the Bonn model was to put meson theory to a real test, no attempt was ever made to minimize the χ^2 of the fit of the NN data. Nevertheless, the Bonn full model shows the smallest χ^2 for the fit of the NN data among the traditional models.

Summary

In Table 1, we give a summary and an overview of the theoretical input of some representative meson-theoretic NN models of the pre-1990 era. Moreover, this table also lists the χ^2/datum for the fit of the world NN data below 300 MeV laboratory energy, which is 5.12, 3.71, and 1.90 for the Nijmegen [11], Paris [14], and Bonn [16] potentials, respectively. This compact presentation, typical for a table, makes it easy to grasp one important point: The more seriously and consistently meson theory is pursued, the better the results. This table and its trend towards the more comprehensive meson models is the best proof for the validity of meson theory in the low-energy nuclear regime. To show this fact, which is of fundamental importance to our field, was the major achievement of the pre-1990 era.

While all models considered in Table 1 describe the proton-proton (pp) data well (with $\chi^2/\text{datum} \approx 2$), some models have a problem with the neutron-proton (np) data (with $\chi^2/\text{datum} \approx 4 - 6$). For the case of the Paris potential (and, in part, for the Nijmegen potential) this is due to a bad reproduction of the np total cross section data. When the latter data are ignored, the Paris potential fits np as well as pp . The Nijmegen and the Paris potential predict too large np total cross sections because their 3D_2 phase shifts are too large [9].

This finishes the review of the developments concerning the NN interaction up to the late 1980's. Next, we turn to the progress made in the 1990's.

RECENT PROGRESS IN NN POTENTIALS

In the 1990's, the focus has been on the quantitative aspect of the NN potentials. Even the best NN models of the past fit the NN data typically with a $\chi^2/\text{datum} \approx 2$ or more. This is still substantially above the perfect $\chi^2/\text{datum} \approx 1$. To put microscopic nuclear structure theory to a reliable test, one needs a perfect NN potential such that discrepancies in the predictions cannot be blamed on a bad fit of the NN data by the potential.

To construct perfect NN potentials one needs, first, a perfect NN analysis. About a decade ago, the Nijmegen group embarked on a program to substantially improve NN phase shift analysis. Finally, in 1993, they could publish a phase-shift analysis of all proton-proton and neutron-proton data below 350 MeV laboratory energy with a χ^2 per datum of 0.99 for 4301 data [17]. Based upon this analysis, new 'high-precision' or 'high-quality' NN potentials have been constructed which, similar to the analysis, fit the NN data with a $\chi^2/\text{datum} \approx 1$.

I will first review the Nijmegen NN analysis and then the new potentials.

The Nijmegen NN Analysis

In spite of the huge NN database available today, conventional phase shift analyses are by no means perfect. For example, the phase shift solutions obtained by Bugg [18] or the VPI group [19] typically have a χ^2/datum of about 1.4, for the energy range 0–425 MeV. This may be due to inconsistencies in the data as well as deficiencies in the constraints applied in the analysis. In any case, it is a matter of fact that within the conventional phase shifts analysis, in which the lower partial waves are essentially unconstrained, a better fit cannot be achieved.

To further improve NN analysis, the Nijmegen group took two decisive measures [17]. First, they 'pruned' the data base; i.e., they scanned very critically the world NN data base (all data in the energy range 0–350 MeV laboratory energy published in a regular physics journal between January 1955 and December 1992) and eliminated all data that had either an improbably high χ^2 (more than three standard deviations off) or an improbably low χ^2 ; of the 2078 world pp data below 350 MeV 1787 survived the scan, and of the 3446 np data 2514 survived. Second, they introduced sophisticated, semi-phenomenological model assumptions into the analysis. Namely, for each of the lower partial waves ($J \leq 4$) a different energy-dependent potential is adjusted to constrain the energy-dependent analysis. Phase shifts are obtained using these potentials in a Schrodinger equation. From these phase shifts the predictions for the observables are calculated including the χ^2 for the fit of the experimental data. This χ^2 is then minimized as a function of the parameters of the partial-wave potentials. Thus, strictly speaking, the Nijmegen analysis is a *potential analysis*; the final phase shifts are the ones predicted by the 'optimized' partial-wave potentials.

In the Nijmegen analysis, each partial-wave potential consists of a short- and a long-range part, with the separation line at $r = 1.4$ fm. The long-range potential V_L ($r > 1.4$ fm) is made up of an electromagnetic part V_{EM} and a nuclear part V_N :

$$V_L = V_{EM} + V_N \quad (1)$$

The electromagnetic interaction can be written as

$$V_{EM}(pp) = V_C + V_{VP} + V_{MM}(pp) \quad (2)$$

for proton-proton scattering and

$$V_{EM}(np) = V_{MM}(np) \quad (3)$$

for neutron-proton scattering, where V_C denotes an improved Coulomb potential (which takes into account the lowest-order relativistic corrections to the static Coulomb potential and includes contributions of all two-photon exchange diagrams); V_{VP} is the vacuum polarization potential, and V_{MM} the magnetic moment interaction.

The nuclear long-range potential V_N consists of the local one-pion-exchange (OPE) tail V_π (the coupling constant g_π being one of the parameters used to minimize the χ^2) multiplied by a factor M/E and the tail of the heavy-boson-exchange (HBE) contributions of the Nijmegen78 potential [11] V_{HBE} , enhanced by a factor of 1.8 in singlet states; i. e.

$$V_N = \frac{M}{E} \times V_\pi(g_\pi, m_\pi) + f(S) \times V_{HBE} \quad (4)$$

with $f(S=0) = 1.8$ and $f(S=1) = 1.0$, where S denotes the total spin of the two-nucleon system. The energy-dependent factor M/E (with $E = \sqrt{M^2 + q_0^2}$, $q_0^2 = MT_{lab}/2$) takes into account relativity in a ‘minimal’ way, damping the nonrelativistic OPE potential at higher energies.

As indicated, V_π depends on the πNN coupling constant g_π and the pion mass m_π , which gives rise to charge dependence. For pp scattering, the OPE potential is

$$V_\pi^{pp} = V_\pi(g_{\pi^0}, m_{\pi^0}) \quad (5)$$

with m_{π^0} the mass of the neutral pion. In np scattering, we have to distinguish between $T=1$ and $T=0$:

$$V_\pi^{np}(T) = -V_\pi(g_{\pi^0}, m_{\pi^0}) + (-1)^{T+1} 2V_\pi(g_{\pi^\pm}, m_{\pi^\pm}) \quad (6)$$

The partial-wave short-range potentials ($r \leq 1.4$ fm) are energy-dependent square-wells (see Figs. 2 and 3 of Ref. [17]). The energy-dependence of the depth of the square-well is parametrized in terms of up to three parameters per partial wave. For the states with $J \leq 4$, there are a total of 39 such parameters (21 for pp and 18 for np) plus the pion-nucleon coupling constants (g_{π^0} and g_{π^\pm}).

In the Nijmegen np analysis, the $T=1$ np phase shifts are calculated from the corresponding pp phase shifts (except in 1S_0 where an independent analysis is conducted) by applying corrections due to electromagnetic effects and charge dependence of OPE. Thus, the np analysis determines $^1S_0(np)$ and the $T=0$ states, only.

In the combined pp and np analysis [17], the fit for 1787 pp data and 2514 np data below 350 MeV results in the ‘perfect’ $\chi^2/\text{datum} = 0.99$.

The New High-Precision NN Potentials

Based upon the Nijmegen analysis and the (pruned) Nijmegen data base, new charge-dependent NN potentials were constructed in the early/mid 1990’s. The groups involved and the names of their new creations are, in chronological order:

- Nijmegen group [20]: Nijm-I, Nijm-II, and Reid93 potentials.
- Argonne group [21]: V_{18} potential.
- Bonn group [22]: CD-Bonn potential.

All these potentials have in common that they use about 45 parameters and fit the pruned Nijmegen data base with a $\chi^2/\text{datum} \approx 1$ (cf. Table 2, below). The larger number of parameters (as compared to previous OBE models) is necessary to achieve the very accurate fit.

Concerning the theoretical basis of these potential, one could say that they are all—more or less—constructed ‘in the spirit of meson theory’ (e.g., all potentials include the one-pion-exchange contribution). However, there are considerable differences in the details leading to considerable off-shell differences among the potentials.

To explain these details and differences in a systematic way, let me first sketch the general scheme for the derivation of a meson-theoretic potential.

One starts from field-theoretic Lagrangians for meson-nucleon coupling, which are essentially fixed by symmetries. Typical examples for such Lagrangians are:

$$\mathcal{L}_{ps} = -g_{ps} \bar{\psi} i \gamma^5 \psi \varphi^{(ps)} \quad (7)$$

$$\mathcal{L}_s = g_s \bar{\psi} \psi \varphi^{(s)} \quad (8)$$

$$\mathcal{L}_v = g_v \bar{\psi} \gamma^\mu \psi \varphi_\mu^{(v)} + \frac{f_v}{4M} \bar{\psi} \sigma^{\mu\nu} \psi (\partial_\mu \varphi_\nu^{(v)} - \partial_\nu \varphi_\mu^{(v)}) \quad (9)$$

where ps , s , and v denote pseudoscalar, scalar, and vector couplings/fields, respectively.

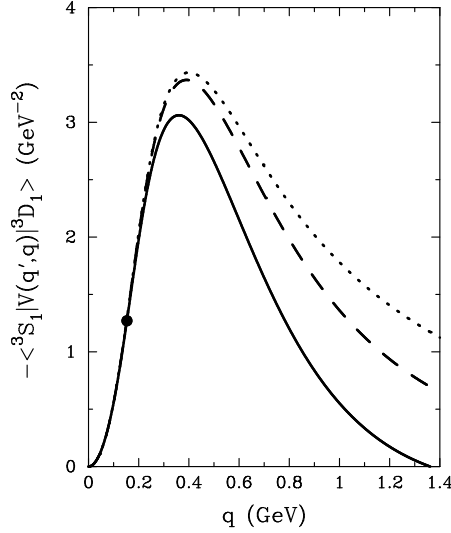


FIGURE 1. Half off-shell 3S_1 - 3D_1 amplitude for the relativistic CD-Bonn potential (solid line), Eq. (11). The dashed curve is obtained when the local approximation, Eq. (13), is used for OPE, and the dotted curve results when this approximation is also used for one- ρ exchange. $q' = 153$ MeV.

The lowest order contributions to the nuclear force from the above Lagrangians are the second-order Feynman diagrams which, in the center-of-mass frame of the two interacting nucleons, produce the amplitude:

$$\mathcal{A}_\alpha(q', q) = \frac{\bar{u}_1(\mathbf{q}')\Gamma_1^{(\alpha)}u_1(\mathbf{q})P_\alpha\bar{u}_2(-\mathbf{q}')\Gamma_2^{(\alpha)}u_2(-\mathbf{q})}{(q' - q)^2 - m_\alpha^2}, \quad (10)$$

where $\Gamma_i^{(\alpha)}$ ($i = 1, 2$) are vertices derived from the above Lagrangians, u_i are Dirac spinors representing the nucleons, and q and q' are the nucleon relative momenta in the initial and final states, respectively; P_α divided by the denominator is the meson propagator.

The simplest meson-exchange model for the nuclear force is the one-boson-exchange (OBE) potential [5] which sums over several second-order diagrams, each representing the single exchange of a different boson, α :

$$V(\mathbf{q}', \mathbf{q}) = \sqrt{\frac{M}{E'}}\sqrt{\frac{M}{E}} \sum_\alpha i\mathcal{A}_\alpha(\mathbf{q}', \mathbf{q})F_\alpha^2(\mathbf{q}', \mathbf{q}). \quad (11)$$

As is customary, we include form factors, $F_\alpha(\mathbf{q}', \mathbf{q})$, applied to the meson-nucleon vertices, and a square-root factor $M/\sqrt{E'E}$ (with $E = \sqrt{M^2 + \mathbf{q}^2}$ and $E' = \sqrt{M^2 + \mathbf{q}'^2}$; M is the nucleon mass). The form factors regularize the amplitudes for large momenta (short distances) and account for the extended structure of nucleons in a phenomenological way. The square root factors make it possible to cast the unitarizing, relativistic, three-dimensional Blankenbecler-Sugar (BbS) equation for the scattering amplitude [a reduced version of the four-dimensional Bethe-Salpeter (BS) equation] into a form which is identical to the (nonrelativistic) Lippmann-Schwinger equation [5]. Thus, Eq. (11) defines a relativistic potential which can be consistently applied in conventional, nonrelativistic nuclear structure.

Clearly, the Feynman amplitudes, Eq. (10), are in general nonlocal expressions; i. e., Fourier transforming them into configuration space will yield functions of r and r' , the relative distances between the two in- and out-going nucleons, respectively. The square root factors create additional nonlocality.

While nonlocality appears quite plausible for heavy vector-meson exchange (corresponding to short distances), we have to stress here that even the one-pion-exchange (OPE) Feynman amplitude is nonlocal. This is important because the pion creates the dominant part of the nuclear tensor force which plays a crucial role in nuclear structure.

Applying $\Gamma^{(\pi)} = g_\pi\gamma_5$ in Eq. (10), yields the Feynman amplitude for neutral pion exchange in pp scattering,

$$i\mathcal{A}_\pi(\mathbf{q}', \mathbf{q}) = -\frac{g_\pi^2}{4M^2} \frac{(E' + M)(E + M)}{(\mathbf{q}' - \mathbf{q})^2 + m_\pi^2} \left(\frac{\boldsymbol{\sigma}_1 \cdot \mathbf{q}'}{E' + M} - \frac{\boldsymbol{\sigma}_1 \cdot \mathbf{q}}{E + M} \right) \times \left(\frac{\boldsymbol{\sigma}_2 \cdot \mathbf{q}'}{E' + M} - \frac{\boldsymbol{\sigma}_2 \cdot \mathbf{q}}{E + M} \right). \quad (12)$$

TABLE 2. Modern high-precision NN potentials and their predictions for the two- and three-nucleon systems.

	CD-Bonn [22]	Nijm-I [20]	Nijm-II [20]	Reid93 [20]	V_{18} [21]	<i>Nature</i>
Character	nonlocal	nonloc. centr. pot. local otherwise	local	local	local	nonlocal
# of parameters	45	41	47	50	40	–
χ^2/datum	1.03	1.03	1.03	1.03	1.09	–
$g_\pi^2/4\pi$	13.6	13.6	13.6	13.6	13.6	14.0(5)
<i>Deuteron properties:</i>						
Quadr. moment (fm ²)	0.270	0.272	0.271	0.270	0.270	0.276(3) ^a
Asymptotic D/S state	0.0255	0.0253	0.0252	0.0251	0.0250	0.0256(4)
D-state probab. (%)	4.83	5.66	5.64	5.70	5.76	–
<i>Triton binding (MeV):</i>						
nonrel. calculation	8.00	7.72	7.62	7.63	7.62	–
relativ. calculation	8.2	–	–	–	–	8.48

^a Corrected for meson-exchange currents and relativity.

This is the original and correct result for OPE.

If one now introduces the drastic approximation,

$$E' \approx E \approx M, \quad (13)$$

then one obtains the momentum space representation of the *local* OPE,

$$V_\pi^{(loc)}(\mathbf{k}) = -\frac{g_\pi^2}{4M^2} \frac{(\boldsymbol{\sigma}_1 \cdot \mathbf{k})(\boldsymbol{\sigma}_2 \cdot \mathbf{k})}{\mathbf{k}^2 + m_\pi^2} \quad (14)$$

with $\mathbf{k} = \mathbf{q}' - \mathbf{q}$. Notice that on-shell, i. e., for $|\mathbf{q}'| = |\mathbf{q}|$, $V_\pi^{(loc)}$ equals $i\mathcal{A}_\pi$. Thus, the nonlocality affects the OPE potential off-shell.

Fourier transform of Eq. (14) yields the well-known local OPE potential in r -space,

$$V_\pi^{(loc)}(\mathbf{r}) = \frac{g_\pi^2}{12\pi} \left(\frac{m_\pi}{2M}\right)^2 \left[\left(\frac{e^{-m_\pi r}}{r} - \frac{4\pi}{m_\pi^2} \delta^{(3)}(\mathbf{r}) \right) \boldsymbol{\sigma}_1 \cdot \boldsymbol{\sigma}_2 + \left(1 + \frac{3}{m_\pi r} + \frac{3}{(m_\pi r)^2} \right) \frac{e^{-m_\pi r}}{r} \mathbf{S}_{12} \right], \quad (15)$$

where m_π denotes the pion mass. Notice, however, that this ‘well-established’ local OPE potential is only an approximative representation of the correct OPE Feynman amplitude. A QED analog is the local Coulomb potential *versus* the full field-theoretic one-photon-exchange Feynman amplitude.

It is now of interest to know by how much the local approximation changes the original amplitude. This is demonstrated in Fig. 1, where the half off-shell 3S_1 - 3D_1 potential, which can be produced only by tensor forces, is shown. The on-shell momentum q' is held fixed at 153 MeV (equivalent to 50 MeV laboratory energy), while the off-shell momentum q runs from zero to 1400 MeV. The on-shell point ($q = 153$ MeV) is marked by a solid dot. The solid curve is the CD-Bonn potential which contains the full, nonlocal OPE amplitude Eq. (12). When the static/local approximation, Eq. (13), is made, the dashed curve is obtained. When this approximation is also used for the one- ρ exchange, the dotted curve results. It is clearly seen that the static/local approximation substantially increases the tensor force off-shell. Clearly, we are dealing here not with negligible effects, and the local approximation is obviously not a good one.

Even though the spirit of the new generation of potentials is more sophistication, only the CD-Bonn potential uses the full, original, nonlocal Feynman amplitude for OPE, Eq. (12), while all other potentials still apply the local approximation, Eqs. (14) and (15). As a consequence of this, the CD-Bonn potential has a weaker tensor force as compared to all other potentials. This is reflected in the predicted D-state probability of the deuteron, P_D , which is due to the nuclear tensor force. While CD-Bonn predicts $P_D = 4.83\%$, the other potentials yield $P_D = 5.7(1)\%$ (cf. Table 2). These differences in the strength of the tensor force lead to considerable differences in the nuclear structure predictions (see discussion below).

The OPE contribution to the nuclear force essentially takes care of the long-range interaction and the tensor force. In addition to this, all models must describe the intermediate and short range interaction, for which very different approaches are taken. The CD-Bonn includes (besides the pion) the pseudoscalar $\eta(549)$ meson, the vector mesons $\rho(769)$ and $\omega(783)$, and two scalar bosons $a_0/\delta(983)$ and $\sigma(550)$, using the full, nonlocal Feynman amplitudes,

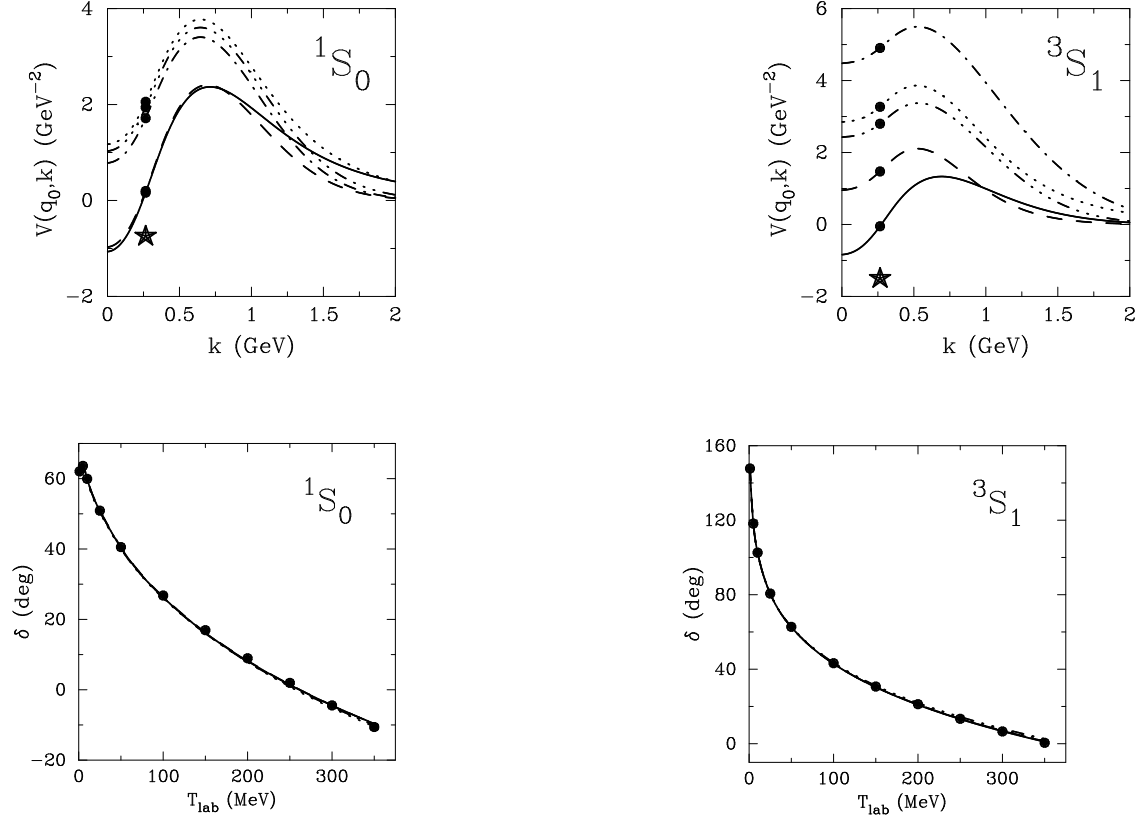


FIGURE 2. Upper part: Matrix elements $V(q_0, k)$ of the 1S_0 and 3S_1 potentials for the CD-Bonn (solid line), Nijm-I (dashed), Nijm-II (dash-dot), Argonne V_{18} (dash-triple-dot) and Reid93 (dotted) potentials. The diagonal matrix elements with $k = q_0 = 265 \text{ MeV}/c$ (equivalent to $T_{\text{lab}} = 150 \text{ MeV}$) are marked by a solid dot. The corresponding matrix element of the full scattering R -matrix is marked by the star. **Lower part:** Predictions for the np phase shifts in the 1S_0 and 3S_1 state by the five potentials. The five curves are essentially indistinguishable. The solid dots represent the Nijmegen multi-energy np analysis [17].

Eq. (10), for their exchanges. Thus, all components of the CD-Bonn are nonlocal and the off-shell behavior is the original one that is determined from relativistic field theory.

The models Nijm-I and Nijm-II are based upon the Nijmegen78 potential [11] (discussed in the historical section above) which is constructed from approximate OBE amplitudes. Whereas the Nijm-I uses the totally local approximations for all OBE contributions, the Nijm-II keeps some nonlocal terms in the central force component (but the Nijm-I tensor force is totally local). Nonlocalities in the central force have only a very moderate impact on nuclear structure as compared to nonlocalities in the tensor force. Thus, if for some reason one wants to keep only some of the original nonlocalities in the nuclear force and not all of them, then it would be more important to keep the tensor force nonlocalities.

The Reid93 [20] and Argonne V_{18} [21] potentials do not use meson-exchange for intermediate and short range; instead, a phenomenological parametrization is chosen. The Argonne V_{18} uses local functions of Woods-Saxon type, while Reid93 applies local Yukawas of multiples of the pion mass, similar to the original Reid potential of 1968 [23]. At very short distances, the potentials are regularized either by exponential (V_{18} , Nijm-I, Nijm-II) or by dipole (Reid93) form factors (which are all local functions).

In Fig. 2, the five high-precision potentials (in momentum space) and their phase shift predictions are shown, for the 1S_0 and 3S_1 states. While the phase shift predictions are indistinguishable, the potentials differ widely—due to the theoretical and mathematical differences discussed. Note that NN potentials differ the most in S -waves and converge with increasing L (where L denotes the total orbital angular momentum of the two-nucleon system).

Before we finish this section, a word about charge dependence is in place. All new potentials are charge-dependent which is essential for obtaining a good χ^2 . Thus, each potential comes in three variants: pp , np , and nn . The difference between pp (without electromagnetic effects) and np is essentially given by the charge dependence of OPE, Eqs. (5) and (6), for states with $L > 0$. However, in the 1S_0 state, this explains only about 50% of the empirically known difference between the pp and np scattering lengths. The remainder is fitted phenomenologically. Also the pp and nn singlet scattering lengths differ, which breaks charge symmetry. The impact of the mass difference between proton and neutron on the kinetic energy and on the OBE amplitudes, alone, does not explain this difference. Therefore, the CD-Bonn and the Argonne V_{18} nn potentials are phenomenologically adjusted to reproduce the nn scattering length (a_{nn}). The potentials by the Nijmegen group (Nijm-I, Nijm-II, Reid93) do not reproduce a_{nn} .

The above discussion reveals that there is still room for improvement concerning the charge dependence of the new high-precision potentials. It is well-known that there are, besides OPE, other mechanisms which create charge dependence of the nuclear force. Recently, the charge dependence and charge asymmetry as created by a comprehensive microscopic model have been calculated carefully [24,25]. A refined version of the CD-Bonn potential [26] which incorporates the results of this comprehensive study is in preparation. To give an idea of how important additional refinements are, we note that the current charge-dependent, high-precision potentials cannot explain the Nolen-Schiffer anomaly [27]. Taking the charge asymmetry derived in Ref [25] into account, however, explains the anomaly correctly [28].

NN POTENTIALS AND NUCLEAR STRUCTURE

Our goal for this section is to understand how the off-shell NN potential influences nuclear structure predictions. For this, we need to discuss first how the NN t -matrix is calculated, since it is an important quantity in the construction of potentials.

For a given NN potential V , the t -matrix for free-space two-nucleon scattering is obtained from the Lippmann-Schwinger equation, which in the center-of-mass (c.m.) frame reads

$$t(\mathbf{q}', \mathbf{q}; E) = V(\mathbf{q}', \mathbf{q}) - \int d^3k V(\mathbf{q}', \mathbf{k}) \frac{M}{k^2 - ME - i\epsilon} t(\mathbf{k}, \mathbf{q}; E) \quad (16)$$

and in partial-wave decomposition

$$t_{L'L}^{JST}(q', q; E) = V_{L'L}^{JST}(q', q) - \sum_{L''} \int_0^\infty k^2 dk V_{L'L''}^{JST}(q', k) \frac{M}{k^2 - ME - i\epsilon} t_{L''L}^{JST}(k, q; E), \quad (17)$$

where \mathbf{q} , \mathbf{k} , and \mathbf{q}' are the relative three-momenta of the two interacting nucleons in the initial, intermediate, and final state; and $q \equiv |\mathbf{q}|$, $k \equiv |\mathbf{k}|$, and $q' \equiv |\mathbf{q}'|$. E denotes the energy of the two interacting nucleons in the c.m. system and is given by

$$E = \frac{q_0^2}{M} \quad (18)$$

with q_0 the magnitude of the initial relative momentum (c.m. on-shell momentum) which is related to the laboratory energy by $T_{lab} = 2q_0^2/M$.

Notice that the integration over the intermediate momenta k in Eqs. (16) and (17) extends from zero to infinity. For intermediate states with $k \neq q_0$, energy is not conserved and the nucleons are off their energy shell ('off-shell'). The off-shell part of the potential (and of the t -matrix) is involved. Thus, in the integral term in Eqs. (16) and (17), the potential (and the t -matrix) contributes off-shell.

Note, however, that in free-space NN scattering, the off-shell potential does not really play a role (it plays a significant role in the few- and many-body problem, see below). The reason for this is simply the procedure by which NN potentials are constructed. The parameters of NN potentials are adjusted so that the resulting on-shell t -matrix fits the empirical NN data. It is important to understand this point, for our later discussion. Therefore, let us consider a case for which the off-shell contributions are particularly large, namely the on-shell t -matrix in the 3S_1 state:

$$\begin{aligned} t_{00}^{110}(q_0, q_0; E) &= V_{00}^{110}(q_0, q_0) - \int_0^\infty k^2 dk V_{00}^{110}(q_0, k) \frac{M}{k^2 - ME - i\epsilon} t_{00}^{110}(k, q_0; E) \\ &\quad - \int_0^\infty k^2 dk V_{02}^{110}(q_0, k) \frac{M}{k^2 - ME - i\epsilon} t_{20}^{110}(k, q_0; E) \end{aligned} \quad (19)$$

Up to second order in V , this is

$$t_{00}^{110}(q_0, q_0; E) \approx V_{00}^{110}(q_0, q_0) - \int_0^\infty k^2 dk V_{00}^{110}(q_0, k) \frac{M}{k^2 - ME - i\epsilon} V_{00}^{110}(k, q_0) \\ - \int_0^\infty k^2 dk V_{02}^{110}(q_0, k) \frac{M}{k^2 - ME - i\epsilon} V_{20}^{110}(k, q_0) \quad (20)$$

$$\approx V_{00}^{110}(q_0, q_0) - \int_0^\infty k^2 dk V_{02}^{110}(q_0, k) \frac{M}{k^2 - ME - i\epsilon} V_{20}^{110}(k, q_0) \quad (21)$$

where in the last equation, we have neglected the second order term in V_{00}^{110} which is, in general, smaller than the second order in V_{02}^{110} . Without partial-wave decomposition,

$$t(\mathbf{q}_0, \mathbf{q}_0; E) \approx V_C(\mathbf{q}_0, \mathbf{q}_0) - \int d^3k V_T(\mathbf{q}_0, \mathbf{k}) \frac{M}{k^2 - ME - i\epsilon} V_T(\mathbf{k}, \mathbf{q}_0), \quad (22)$$

where V_C denotes the central force and V_T the tensor force. In words: the most important contributions are the central force in lowest order and the tensor force in second order.

The on-shell t -matrix is related to the observables that are measured in experiments. Thus potentials which fit the same NN scattering data produce the same on-shell t -matrices. However, this does not imply that the potentials are the same. As seen in Eqs. (16) and (17), the t -matrix is the sum of two terms: the Born term and an integral term. When this sum is the same, the individual terms may still be quite different.

As an example, we pick up again the case of the 3S_1 state, which is attractive below 300 MeV laboratory energy. Instead of using the t -matrix, it is more convenient to consider the (real) K -matrix (denoted by R below) which, similar to Eq. (19), is given by,

$$R_{00}^{110}(q_0, q_0; E) = V_{00}^{110}(q_0, q_0) - \mathcal{P} \int_0^\infty k^2 dk V_{00}^{110}(q_0, k) \frac{M}{k^2 - ME} R_{00}^{110}(k, q_0; E) \\ - \mathcal{P} \int_0^\infty k^2 dk V_{02}^{110}(q_0, k) \frac{M}{k^2 - ME} R_{20}^{110}(k, q_0; E), \quad (23)$$

where \mathcal{P} denotes the principal value integral.

In Fig. 2 (upper part), the on-shell R matrix, $R(q_0, q_0; E)$, which corresponds to the empirical phase shift, is denoted by a star and the potential Born term, $V(q_0, q_0)$ is given by a solid dot, for each potential. The difference between star and dot is due to the integral term. Clearly, the size of the integral term (in which the off-shell potential is involved) is very different for different potentials. Hard and strong-tensor-force potentials produce large integral terms, while soft and weak-tensor-force potentials produce small integral terms. Note, however, that by construction the Born and integral terms are balanced such that the same result is obtained for $R(q_0, q_0; E)$ (the star in Fig. 2 is the same for all potentials).

Let us now turn to the many-body problem and consider first the three-nucleon system. The most important point to notice here is that a two-nucleon t -matrix is the input for the three-body Faddeev equations. However, the energy parameter E for this two-body t -matrix is different from the one used in free-space scattering. In the three-body Faddeev equations, one uses

$$E = -B_t - \frac{3}{4} \frac{q^2}{M} \quad (24)$$

where B_t (≈ 8.5 MeV) is the triton binding energy and q is the magnitude of the momentum of the spectator nucleon. Notice that the energy parameter E is negative here, in contrast to free scattering where E is positive. In a Faddeev calculation, q runs from zero to infinity; thus, the parametric energy for the two-body t -matrix ranges between ≈ -8.5 MeV and $-\infty$. Inspection of Eq. (16) reveals that this negative energy parameter will quench the integral term of the Lippmann-Schwinger equation due to an increase of the energy-denominator. Since this integral term is attractive, the t -matrix will become less attractive as a result of this quenching. This effect will be particularly large for the t -matrix in the 3S_1 state, Eq. (19). The consequence is that potentials with large integral terms (i. e., hard potentials, large P_D), will experience more quenching of the attractive integral term and, thus, lose more attraction than potentials with a small integral term (soft potentials).

These arguments can also be stated in more intuitive form. All NN potentials reproduce the deuteron binding energy. In the deuteron, the tensor force couples the 3S_1 to the 3D_1 state. The triton is a much smaller system than the deuteron. Therefore, in the triton, the D -state is located at much higher energy than in the deuteron. This

TABLE 3. Predictions by some high-precision NN potentials for the energy per nucleon in nuclear matter (in units of MeV) at $k_F = 1.35 \text{ fm}^{-1}$. The contributions from some important partial waves and the totals are given.

	CD-Bonn	Nijm-I	Nijm-II
1S_0	-16.75	-16.73	-16.11
3S_1	-19.00	-17.55	-17.05
3P_0	-3.09	-3.11	-3.06
3P_1	9.84	9.73	9.72
3P_2	-7.03	-7.00	-7.01
Total potential energy	-36.35	-35.07	-33.70
Kinetic energy	22.67	22.67	22.67
Total energy	-13.68	-12.40	-11.02

increases the energy gap between the S and D states and makes an S - D transition via the tensor force less likely in the denser system [29]. This ‘medium effect’ on the second order tensor contribution [cf. Eq. (22)] reduces the binding energy. The stronger the tensor force, the larger the reduction.

This dependence of the triton binding energy predictions on the off-shell potential, particularly the off-shell tensor potential, is confirmed by the results shown in the lower part of Table 2. In a charge-dependent 34-channel momentum-space Faddeev calculation, one obtains 8.00 MeV using the CD-Bonn potential and 7.62(1) MeV applying any of the local potentials. This difference of 0.38 MeV is due to the off-shell differences between the local and nonlocal potentials.

The unacquainted observer may be tempted to believe that this difference of 0.38 MeV is quite small, almost negligible. This is not true. The discrepancy between the predictions of local potentials (7.62 MeV) and experiment (8.48 MeV) is 0.86 MeV. Thus, the problem with the triton binding is that 0.86 MeV cannot be explained in the simplest way, that is all. Any non-trivial contribution must, therefore, be measured against the 0.86 MeV gap between experiment and the simplest theory. On this scale, the nonlocality of the CD-Bonn explains almost 50% of the gap; i. e., it is substantial.

Concerning the remaining difference between theory and experiment, two comments are appropriate. First, besides the relativistic, nonlocal effects that can be absorbed into the two-body potential concept [Eq. (11)], there are further relativistic corrections that come from a relativistic treatment of the three-body system. This increases the triton binding energy by 0.2–0.3 MeV [30–32,22]. Second, notice that the present nonlocal potentials include only the nonlocalities that come from meson-exchange. However, the composite structure (quark substructure) of hadrons should provide additional nonlocalities which may be even larger. It is a challenging topic for future research to derive these additional nonlocalities, and test their impact on nuclear structure predictions.

For heavier systems, the Brueckner G -matrix is the basic quantity for all calculations of nuclear ground and excited states. The G -matrix is the solution of the Bethe-Goldstone equation,

$$G(\mathbf{q}', \mathbf{q}) = V(\mathbf{q}', \mathbf{q}) - \int d^3k V(\mathbf{q}', \mathbf{k}) \frac{M^* Q}{k^2 - q^2} G(\mathbf{k}, \mathbf{q}) , \quad (25)$$

which differs from the Lippmann-Schwinger equation, Eq. (16), in two points: the Pauli projector Q and the energy denominator. (For simplicity, I assume in Eq. (25) the so-called continuous choice for the single particle energies in nuclear matter, i. e., the energy of a nucleon is represented by $\epsilon(p) = p^2/(2M^*) - U_0$ for $p \leq k_F$ as well as $p > k_F$, where M^* is the effective mass and U_0 a positive constant.) The Pauli projector prevents scattering into occupied states and, thus, cuts out the low momenta in the k integration. The change introduced by the Pauli projector is known as the Pauli effect. The energy denominator gives rise to the so-called dispersive effect. When using the continuous choice, the dispersive effect is given simply by the replacement of M by M^* ($\approx \frac{2}{3}M$ at nuclear matter density) in the numerator of the integral term, which leads to a reduction of this attractive term by a factor M^*/M . Both effects are in the same direction, namely they quench the integral term. Since the integral term is negative, these effects are repulsive.

In Table 3, nuclear matter results are given for three representative high-precision potentials using the Brueckner pair approximation and the conventional choice for the single particle potential. For the reasons discussed, the largest difference between the predictions occurs in the 3S_1 state where the tensor force is involved. In the 1S_0 state, only the central force can contribute which is nonlocal for CD-Bonn and Nijm-I. This explains why the binding energy predicted for this state is the same for these two potentials, and is larger than the value predicted by the local potential Nijm-II.

Note that there are further contributions in nuclear matter beyond the Brueckner pair approximation. Three- and four-body clusters contribute about 4 MeV attraction [33] and the medium effect on the Dirac spinors representing

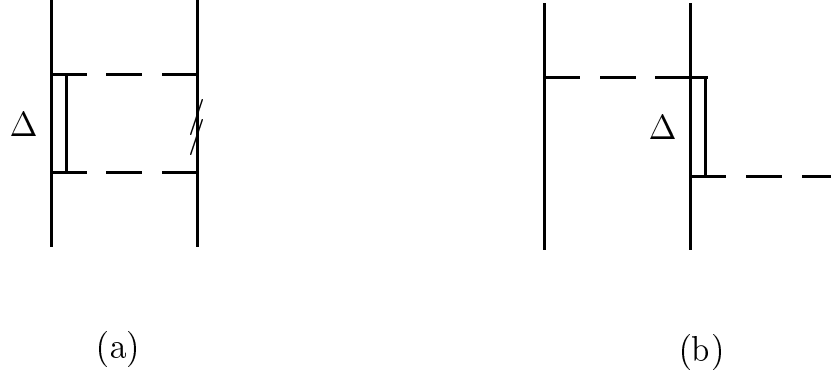


FIGURE 3. Two- and three-body forces created by the Δ isobar. Solid lines represent nucleons, double lines Δ isobars, and dashed lines π and ρ exchange. **Part (a)** is a contribution to the two-nucleon force. The double slash on the intermediate nucleon line is to indicate the medium modifications (Pauli blocking and dispersion effects) that occur when this diagram is inserted into a nuclear many-body environment. **Part (b)** is a three-nucleon force.

the nucleons in nuclear matter creates about 2 MeV repulsion [5] resulting in a net correction of about -2 MeV. This brings the prediction of the nonlocal potential into good agreement with the empirical nuclear matter value of -16 ± 1 MeV.

The trend of the nonlocal Bonn potential to increase binding energies has also a very favorable impact on predictions for spectra of open-shell nuclei [34,35].

THREE-NUCLEON FORCES

Strictly speaking, most many-body forces are an artifact of theory. They are created by ‘freezing out’ degrees of freedom contained in the full Hamiltonian of the problem. This fact allows us to derive a guideline for dealing with the many-body-force issue in a consistent way: when you introduce a new degree of freedom, do not freeze it out; instead take it into account in the two- *and* many-body problem, consistently. Field-theoretic models for the 2π -exchange contribution to the NN interaction require the $\Delta(1232)$ isobar, which also creates a three-nucleon force (3NF) in the many-body system. Consequently, when introducing the isobar degree of freedom, it should be included in the two- and three-body force simultaneously. When these forces are applied in the many-body problem, then one is faced with two effects: a (repulsive) medium effect on the two-body force [Fig. 3(a)] and an attractive 3NF contribution [Fig 3(b)]. The repulsive medium effect has been known for more than 20 years [39]. *Consistency requires that either both effects are taken into account or none.* Consistent calculations of this kind have first been conducted by the Hannover group [36] for the triton. Recently, these calculations have been improved and extended by Picklesimer and coworkers [37] using the Argonne V_{28} Δ -model [38]. They find an attractive contribution to the triton energy of -0.66 MeV from the 3NF diagrams created by the Δ , and a repulsive contribution of $+1.08$ MeV from the dispersive effect on the two-nucleon force involving Δ isobars. The total result is *0.42 MeV repulsion* [37].

A contribution that is missing in the Δ 3NF model is the S-wave part of the off-shell πN amplitude. Estimates for this contribution vary between -0.2 and -0.6 MeV [40]. Adding this to the Argonne V_{28} result [i. e., $0.42 - (0.4 \pm 0.2) = 0.0 \pm 0.2$ MeV] yields a vanishing result for the total contribution from three-body forces.

In the more traditional calculations, it was customary to employ the so-called 2π -exchange three-nucleon force. This approach does not take the dispersive effects into account and overbinds the triton, at least if commonly accepted values for the cut-off parameter of the strong pion-nucleon vertex are used. Moreover, this type of 3N force fails in 3N scattering [41] casting additional doubt on its reality.

Besides the Δ -isobar, there are other mechanisms that can give rise to three-nucleon forces. In recent years, it has become fashionable to consider chiral Lagrangians for nuclear interactions. Such Lagrangians may create diagrams which represent effective three-nucleon potentials. However, Weinberg has shown that all these diagrams cancel [42].

In conclusion, any *consistent* three-body force calculation—conducted to date—has yielded vanishing results. This implies that the two-body force should provide essentially all binding energies observed in nuclei. The further implication then is that nonlocal/weak-tensor force NN interactions are to be favored over hard/local potentials. It

is probably not just an accident that these soft/nonlocal potentials are also more faithful to the underlying theory of nuclear forces.

SUMMARY AND OUTLOOK

Several high-quality/high-precision NN potentials are now available which fit the low-energy NN data with identical perfection. These potentials differ, however, in their off-shell behavior. Thus, the stage is set for a reliable investigation of off-shell effects in microscopic nuclear structure calculations. Such calculations may finally teach us something about the off-shell nature of the nuclear force.

This is *the* time to do *microscopic* nuclear structure calculations!

ACKNOWLEDGEMENT

This work was supported in part by the U.S. National Science Foundation under Grant-No. PHY-9603097.

REFERENCES

1. S. Weinberg, *Physica* **96A**, 327 (1979).
2. S.C. Pieper, contribution to these Proceedings.
3. T.T.S. Kuo and E. Osnes, *Folded-Diagram Theory of the Effective Interaction in Atomic Nuclei*, Springer Lecture Notes in Physics, Vol. 364 (Springer, Berlin, 1990).
4. M. Hjorth-Jensen, T.T.S. Kuo, and E. Osnes, *Phys. Reports* **261**, 125 (1995).
5. R. Machleidt, *Adv. Nucl. Phys.* **19**, 189 (1989).
6. R. Machleidt and G. Q. Li, *Nucleon-nucleon potentials in comparison: Physics or polemics?*, *Phys. Reports* **242**, 5 (1994).
7. R. Bryan and B. L. Scott, *Phys. Rev.* **177**, 1435 (1969).
8. Particle Data Group, *Review of Particle Physics*, *Phys. Rev. D* **54**, 1 (1996), see pp. 329, 355, and 356 therein; *Eur. Phys. J. C* **3**, 1-794 (1998), see p. 363 and pp. 390-392 therein.
9. A more detailed discussion of this issue and figures illustrating the facts can be found in Ref. [6].
10. A. Gersten, R. Thompson, and A. E. S. Green, *Phys. Rev. D* **3**, 2076 (1971); G. Schierholz, *Nucl. Phys.* **B40**, 335 (1972); K. Erkelenz, *Phys. Reports* **13C**, 191 (1974); K. Holinde and R. Machleidt, *Nucl. Phys.* **A247**, 495 (1975), *ibid.* **A256**, 479 (1976); J. Fleischer and J. A. Tjon, *Nucl. Phys.* **B84**, 375 (1975), *Phys. Rev. D* **24**, 87 (1980).
11. M. M. Nagels, T. A. Rijken, and J. J. de Swart, *Phys. Rev. D* **17**, 768 (1978).
12. M. Chemtob, J. W. Durso, and D. O. Riska, *Nucl. Phys.* **B38**, 141 (1972); A. D. Jackson, D. O. Riska, and B. Verwest, *Nucl. Phys.* **A249**, 397 (1975); G. E. Brown and A. D. Jackson, *The Nucleon-Nucleon Interaction* (North-Holland, Amsterdam, 1976).
13. R. Vinh Mau, J. M. Richard, B. Loiseau, M. Lacombe, and W. N. Cottingham, *Phys. Lett.* **B44**, 1 (1973); R. Vinh Mau, in *Mesons in Nuclei*, ed. M. Rho and D. H. Wilkinson (North-Holland, Amsterdam, 1979), p. 151.
14. M. Lacombe, B. Loiseau, J. M. Richard, R. Vinh Mau, J. Côté, P. Pirès, and R. de Tourreil, *Phys. Rev. C* **21**, 861 (1980).
15. J. W. Durso, A. D. Jackson, and B. J. VerWest, *Nucl. Phys.* **A345**, 471 (1980).
16. R. Machleidt, K. Holinde, and Ch. Elster, *Phys. Reports* **149**, 1 (1987).
17. V. G. J. Stoks, R. A. M. Klomp, M. C. M. Rentmeester, and J. J. de Swart, *Phys. Rev. C* **48**, 792 (1993).
18. D. V. Bugg and R. A. Bryan, *Nucl. Phys.* **A540**, 449 (1992).
19. R. A. Arndt *et al.*, *Phys. Rev. D* **45**, 3995 (1992).
20. V. G. J. Stoks, R. A. M. Klomp, C. P. F. Terheggen, and J. J. de Swart, *Phys. Rev. C* **49**, 2950 (1994).
21. R. B. Wiringa, V. G. J. Stoks, and R. Schiavilla, *Phys. Rev. C* **51**, 38 (1995).
22. R. Machleidt, F. Sammarruca, and Y. Song, *Phys. Rev. C* **53**, 1483 (1996).
23. R. V. Reid, *Ann. Phys. (N.Y.)* **50**, 411 (1968).
24. G. Q. Li and R. Machleidt, *Charge-Dependence of the Nucleon-Nucleon Interaction*, *Phys. Rev. C*, in press; nucl-th/9807080.
25. G. Q. Li and R. Machleidt, *Charge-Asymmetry of the Nucleon-Nucleon Interaction*, *Phys. Rev. C*, in press; nucl-th/9804023.
26. R. Machleidt, to be published.
27. J. A. Nolen and J. P. Schiffer, *Annu. Rev. Nucl. Sci.* **19**, 471 (1969).
28. H. Müther, A. Polls, and R. Machleidt, *Isospin symmetry breaking nucleon-nucleon potentials and nuclear structure*, submitted to *Phys. Lett. B*; nucl-th/9809016.
29. D. R. Inglis, *Phys. Rev.* **55**, 988 (1939); R. L. Pease and H. Feshbach, *Phys. Rev.* **88**, 945 (1952).
30. F. Sammarruca, D. P. Xu, and R. Machleidt, *Phys. Rev. C* **46**, 1636 (1992).

31. G. Rupp and J. A. Tjon, Phys. Rev. C **45**, 2133 (1992).
32. F. Sammarruca and R. Machleidt, Few-Body Systems **24**, 87 (1998).
33. H. Q. Song, M. Baldo, G. Giansiracusa, and U. Lombardo, Phys. Rev. Lett. **81**, 1584 (1998).
34. M. F. Jiang, R. Machleidt, D. B. Stout, and T. T. S. Kuo, Phys. Rev. C **46**, 910 (1992).
35. F. Andreozzi *et al.*, Phys. Rev. C **54**, 1636 (1996); A. Covello, contribution to these Proceedings.
36. C. Hajduk, P. U. Sauer, and W. Strueve, Nucl. Phys. **A405**, 581 (1983).
37. A. Picklesimer, R. A. Rice, and R. Brandenburg, Phys. Rev. C **45**, 2045, 2624 (1992); *ibid.* **46**, 1178 (1992).
38. R. B. Wiringa, R. A. Smith, and T. L. Ainsworth, Phys. Rev. C **29**, 1207 (1984).
39. K. Holinde and R. Machleidt, Nucl. Phys. **A280**, 429 (1977).
40. J. L. Friar, B. F. Gibson, G. L. Payne, and S. A. Coon, Few-Body Systems **5**, 13 (1988).
41. H. Witala, D. Hüber, and W. Glöckle, Phys. Rev. C **49**, 14 (1994).
42. S. Weinberg, Phys. Lett. **B251**, 288 (1990); Nucl. Phys. **B363**, 3 (1991); Phys. Lett. **B295**, 114 (1992).